Extended Abstracts of the 2018 International Conference on Solid State Devices and Materials, Tokyo, 2018, pp125-126

XPS Study of Chemical Bonding Features & Inner Potential at Y_2O_3/SiO_2 Interfaces

Nobuyuki Fujimura[1], Akio Ohta[1,2], Mitsuhisa Ikeda[1], Katsunori Makihara[1], and Seiichi Miyazaki[1]

[1] Graduate School of Engineering, Nagoya University Furo-cho Chikusa-ku, Nagoya, 464-8603, Japan
Phone: +81-52-789-2727, E-mail: fujimura.nobuyuki@b.mbox.nagoya-u.ac.jp
[2] Institute for Advanced Research, Nagoya University Furo-cho Chikusa-ku, Nagoya, 464-8601, Japan

Abstract

Chemical reaction at ultrathin Y_2O_3/SiO_2 interface by annealing have been evaluated by XPS analysis. And, impact of YSi_xO_y formation on the electrical dipole moment at the interface have been investigated.

1. Introduction

A clear understanding of inner potential changes at hetero-interfaces in high-k dielectric/metal gate stack is one of crucial issues from a viewpoint of precise tuning of threshold voltage for advanced MISFETs. So far, it has been reported that metallic bonding states [1], oxygen density difference [2], electronegativity [3], dielectric contact induced gap states [4], and oxygen vacancies [5] are discussed as the possible cause of inner potential change by electrical dipole. To get an insight into electrical dipole formation, characterization of chemical structure and bonding features is indispensable. In our previous work [6], it has been reported that electrical dipole moment at the ultrathin high-k/SiO_2 interface and its correlation with the atomic density difference at the interface have been directly evaluated from the XPS analysis. For the high-k(HfO_2, Al_2O_3, and TiO_2)/SiO_2 stack with abrupt interface, the magnitude of these electrical dipole was found to be a liner relationship to the measured oxygen areal density ratio of high-k to SiO_2. On the other hand, negative electrical dipole at high-k(Y_2O_3 and SrO)/SiO_2 interface was not linearly changed against oxygen density ratio by the silicate formation at the interface. Therefore, the purpose of this work is to get a better understanding of influence of silicate formation at Y_2O_3/SiO_2 interface on electrical dipole moment. Changes in the chemical structure and inner potential of Y_2O_3/SiO_2 with thermal annealing have been systematically evaluated by XPS measurements.

2. Experimental Procedure

After a wet chemical cleaning of p-type Si(100) substrate with $NH_4OH : H_2O_2 : H_2O = 0.15 : 3 : 7$ solution at 80 ºC for 10 min, the Si surface was terminated with hydrogen in 4.5% HF solution. Then, the dry oxidation in pure O_2 was conducted for the growth of a ~200 nm-thick SiO_2 layer. In some samples, Y_2O_3 thin film with a thickness of 0.6 ~ 2.0 nm was deposited on thermally-grown SiO_2/Si by the magnetron sputtering, in which the Ar/O_2 gas flow ratio and the power density kept constant at unity and 1.52 W/cm^2, respectively. Then, post deposition annealing was performed at the temperature in the range from 400ºC to 800ºC in dry-N_2 for 5 min to densify the dielectric layers. Uniform coverage with ultrathin Y_2O_3 and flat surface after annealing were also confirmed by AFM measurements as shown in Fig. 1. Chemical bonding features at Y_2O_3/SiO_2 interface were evaluated from XPS measurements under monochromatized AlKα radiation (hν = 1486.6eV). And, inner potential change at Y_2O_3/SiO_2 interface such as interfacial electrical dipole was evaluated from the cut-off energy of secondary photoelectrons (SEs) [6], which corresponds to the vacuum level difference caused by the abrupt potential change.

3. Results and Discussion

Figure 2 shows Y 3d and Si $2p_{3/2}$ core-line spectra taken for a 0.6 nm-thick Y_2O_3/SiO_2 structure before and after annealing at 800 ºC. In each spectrum, the binding energy was calibrated by Si $2p_{3/2}$ signals originated from the thermally-grown SiO_2 to eliminate the energy shift due to the charge up effect during measurements. Y 3d signals were chemically shifted by 0.4 eV toward the higher binding energy side after the annealing at 800 ºC, which indicating the diffusion and incorporation of Y ions into the SiO_2 network, in other words, Y-silicate (YSi_xO_y) formation. Si $2p_{3/2}$ signals were broadened by Y_2O_3 deposition on SiO_2, and the spectral width were slightly decreased after the annealing at 800 ºC. These changes can be responsible for the generation of defects at SiO_2 surface by the sputtering damage during the Y_2O_3 deposition and formation of YSi_xO_y by the annealing. Depth profile of Y ions and YSi_xO_y formation were also confirmed from the take-off angle dependence of XPS signals. It was found that, after the annealing of the 0.6 nm-thick Y_2O_3/SiO_2 at the temperature below 400 ºC, Y_2O_3 layer remain on the surface. In addition, YSi_xO_y with Y/(Si+Y) ratio of 35% was formed on SiO_2 as a result of the chemical reaction of 0.6 nm-thick Y_2O_3 with SiO_2 by the annealing at 600 ºC and 800 ºC.

To investigate the influence of inner potential change in the region near the interface on the silicate formation, the spectrum of SEs were measured before and after the annealing of Y_2O_3/SiO_2 structure as shown in Figs. 3 and 4. In Fig. 3, a spectrum of thermally-grown SiO_2 was also shown as a reference. The SEs for the samples after Y_2O_3 deposition and annealing at 400 ºC were shifted toward the lower kinetic energy side from the reference signals of thermally-grown SiO_2, which indicates the formation of positive fixed charge and/or positive dipole in the region near the Y_2O_3/SiO_2 interface. This is probably due to the sputtering damages as discussed from XPS analysis and/or moisture absorption of Y_2O_3. After the annealing at 600 ºC and 800 ºC, the cut-off energy of SE was close to that of SiO_2. And, for the sample after annealing at 600 ºC, Y_2O_3 thickness dependence of cut-off energy of SEs was hardly detected in the range below 1 nm. From these results, the observed energy shift of SEs is attributable to the abrupt potential change and the presence of negative dipoles at $YSiO_x/SiO_2$ interface. In addition, to check the effect of moisture

absorption in Y_2O_3 to the 600 ºC annealed samples were exposed the air exposure. After air exposure, cut-off energy was shifted toward lower kinetic energy side, which implying the generation of positive fixed charge in the YSi_xO_y.

Next, atomic density of YSi_xO_y layer on SiO_2 was estimated from measures cation core-lineas follows,

$$\frac{n_{top}}{n_{bottom}} = \frac{\lambda_{bottom}}{\lambda_{top}} \times \frac{\sigma_{bottom}}{\sigma_{top}} \times \frac{I_{top}}{I_{bottom}} \times \frac{1}{exp\left(\frac{d_{top}}{\lambda_{top}\sin\theta}\right) - 1}$$

where n, σ, λ, and d is the atomic density, photo-ionized cross section, photoelectron escape depth for photoelectrons, respectively. I_{top} and I_{bottom} was set at the integrated intensities of Y 3d from YSi_xO_y and Si $2p_{3/2}$ from underlying SiO_2, respectively. In the calculation, SiO_2 component was obtained by the spectrum deconvolution of Si $2p_{3/2}$ spectrum. Because the calculated result is corresponding to the cation density ratio, conversion to the oxygen density ratio was carried out in consideration of chemical composition of YSi_xO_y. Obtained oxygen density ratio of high-k dielectrics to SiO_2 was plotted as a function of high-k thickness as shown in Fig. 5. It was found that the electrical dipole moment was linearly changed against oxygen areal density ratio.

In summary, $YSiO_x$ with Y/(Si+Y) composition of 35% was formed after annealing at 600 ºC and 800 ºC, and negative interfacial dipole as small as ~ 0.05 eV was detected. It was suggested that positive fixed charge and/or positive dipole may be generated in the region near the Y_2O_3/SiO_2 interface due to moisture absorption and sputtering damage to the SiO_2 layer. Calculated oxygen density in consideration of the Y/(Si+Y) composition shows a linear relationship with dipole moment.

References [1] T. Nakayama et al., ECS Trans., **3** (2006) 129. [2] K. Kita et al., APL, **94** (2009)132902. [3] L. Lin et al., JAP, **109** (2011) 094502. [4] X. Wang et al., APL, **96** (2010) 152907. [5] Y. Akasaka et al., JJAP, **45** (2006) L1289. [6] N. Fujimura et al., JJAP, **57** (2018) 04FB07.

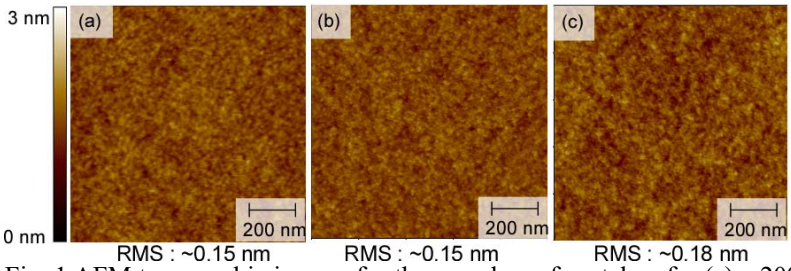

Fig. 1 AFM topographic images for the sample surface taken for (a) a 200 nm-thick thermally-grown $SiO_2/Si(100)$ and a 0.6 nm-thick $Y_2O_3/SiO_2/Si(100)$ (b) before and (c) after annealing at 800 ºC for 5 min.

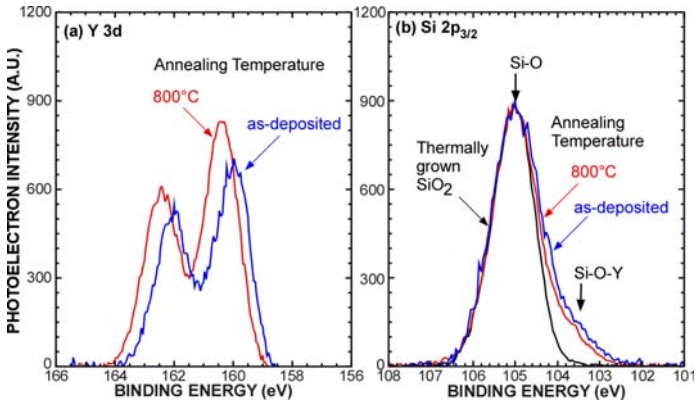

Fig. 2 Y 3d and Si $2p_{3/2}$ spectra taken for a 0.6 nm-thick $Y_2O_3/SiO_2/Si(100)$ before and after annealing at 800 ºC. In each spectrum, photoelectron take-off angle was set at 90º.

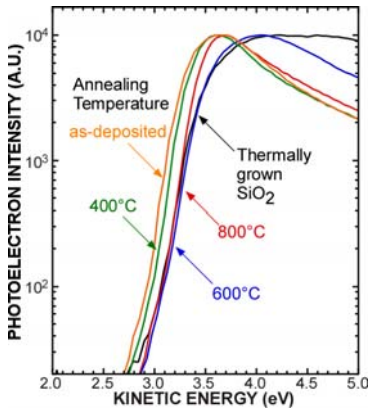

Fig. 3 The yield spectra of secondary photoelectrons taken for thermally-grown SiO_2 and high-k/SiO_2 stack at a photoelectron take-off angle of 90º.

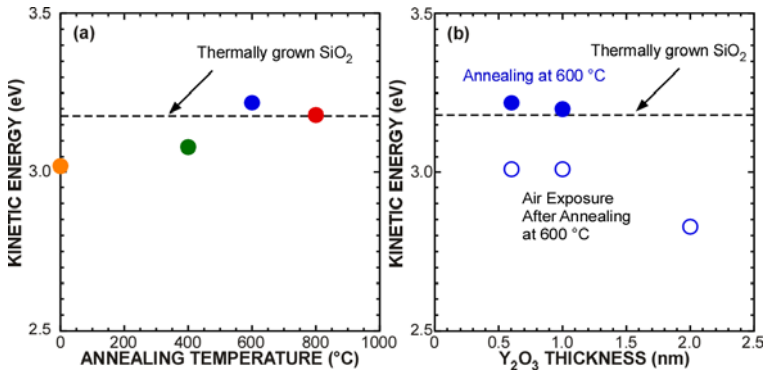

Fig. 4 Cut-off energy of secondary photoelectrons taken for (a) Y_2O_3/SiO_2 stacks after annealing at different temperatures and (b) 600 ºC annealed samples with different high-k thicknesses.

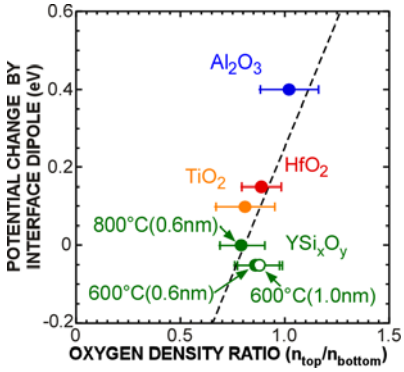

Fig. 5 Electrical dipole moment at YSi_xO_y/SiO_2 interface as a function of oxygen density ratio of YSi_xO_y to SiO_2. Results of HfO_2, Al_2O_3, and TiO_2 were also shown as reference [6].